Deep Learning-based Artificial Intelligence Improves Accuracy of Error-prone Lung Nodules

[1]S. Nagamani, Associate Prof, CSE, nagamanikunchipudi@gmail.com

Swarna Bharathi Institute of Science and Technology

[2]Dr.M.padmavathi , Assoc..prof , CSE,macherlapadmavathi@gmail.com

Swarna Bharathi Institute of Science and Technology

[3] I.Ramesh babu ,Asst prof, CSE, inapala.ramesh35@gmail.com

Swarna Bharathi Institute of Science and Technology

Abstract

In order to enhance outcomes, it is important to discover lung cancer early. It is critical to enhance the ability of chest CT scans to identify nodules. Prior AI modules have shown promising results, leading to better performance in recognizing lung lesions in some datasets. Having said that, their false-positive (FP) rate is really high. No definitive evidence of its efficacy in clinical practice exists at this time. The goal of our AI-assisted CT scans was to reduce FP. Procedures and materials: Obtaining CT scans from sixty patients was the goal. This research aimed to identify lung nodules in five senior physicians who were not told about these patients. Without the use of AI, two medical professionals identified and labeled lung nodules by hand. Three other physicians identified and classified lung nodules with the help of AI before interpreting the results by hand. The artificial intelligence software uses a deep learning architecture. The findings show that 266 nodules were detected. The sensitivity ranged from 59.2% to 67.0% and the FP was 0.617 to 0.650/scan for clinicians who did not use AI. With AI help, physicians' sensitivity ranged from 59.2–77.3% and FP was 0.067–0.2/scan. The use of this AI-powered application greatly decreased FP. Central placement, ground-glass look, and tiny size were the error-prone features of lung nodules. The AI-enhanced software enhanced the identification of nodules that are prone to mistakes. In summary: In order to treat lung cancer, it is crucial to detect nodules in the lungs. Nodules that are prone to errors provide a significant issue for clinicians when dealing with a high volume of CT images. Lung nodule detection performance was enhanced by the AI-assisted algorithm, particularly for nodules that are prone to errors.

Introduction

Among all cancers, lung cancer is a major killer on a global scale [1]. The lung cancer prognosis is highly dependent on tumor stage.Patients diagnosed with lung cancer have just one curative therapy option: surgery [2]. The survival rate is greater for patients whose lung cancer is caught at an operable stage compared to those whose illness has spread. Consequently, it is critical to recognize early signs of lung cancer [1].It is still difficult to diagnose and treat early stage lung cancer. The majority of lung cancer diagnoses are still made with chest CT scans [3]. Lung nodule detection using chest computed tomography images could be useful for doctors.Identify lung cancer in its early stages. Searches for lung nodules on chest computed tomography images as a means of early detection of lung cancer have received a lot of attention [1]. Chest computed tomography (CT) scans for the detection of lung nodules could lead to the early detection of lung cancer and an improved prognosis. If lung nodules can be detected early on, it might lead to the early diagnosis of lung cancer, which could improve the prognosis for individuals with lung cancer and lower healthcare expenses.The problem is that identifying many CT images manually is laborious, attention-requiring, time-consuming, and error-prone.In addition, even for highly trained medical professionals, lung nodules may be a real challenge to detect. Rapid benefits and intriguing advancements in imaging diagnostics have been made possible by artificial intelligence (AI).So, a lot of research has focused on using AI to find lung nodules. Lung nodule detection accuracy has been the target of these efforts [1]. The use of artificial intelligence has enormous promise for enhancing the CT-based diagnosis of lung nodules. When it

came to identifying lung nodules in specific datasets, some of the systems did really well. On the other hand, there is insufficient evidence to confirm its efficacy in clinical practice [1]. No one can really use it in clinical practice because of its poor sensitivity or high false-positive rate [1].Thus, more investigation into the potential uses of AI in healthcare is required.As a result, we are now investigating ways to improve the accuracy of CT scan detection of lung nodules by using computer-aided diagnostic tools that are based on artificial intelligence.

Materials and methods

CT acquisition and reading

In order to identify lung nodules, CT scans of 60 patients were acquired. Using a 64-slice detector, GE LightSpeed, the chest CT scan was conducted with a 2.5 mm lung window slice thickness. The research for the diagnosis of lung nodules included five senior doctors—three chest physicians, one chest surgeon, and one radiology—all with over a decade of expertise in interpreting chest CT images. The physicians were completely unaware of all these situations. Without the use of artificial intelligence, two physicians (doctors 1 and 2) used the conventional approach of manually detecting and categorizing lung nodules.Before human interpretation, three more physicians (doctors 3, 4, and 5) used AI to identify and classify lung nodules. The research was given the go light by the Institutional Review Board of the Buddhist Tzu Chi Medical Foundation, Taipei Tzu Chi Hospital (Protocol Number: 09-X-007).

Setting and Notations of AI algorithm

$$\mathbb{H} = \{H_i = (p_i, d_i)\}_{i=1}^{N}$$

$$p_i = (x_i, y_i, z_i) \in \mathbb{R}^3 \; d_i$$

$$\mathbb{H}$$

$$y \in \{0,1\}$$

In a 3D CT scan of the lungs (image I) with N nodules, we represent the set of nodules as, and the spatial position and diameter of the ith nodule are denoted as $\{z1, z2, \ldots, zБn, n \leq k\}$. It is not possible to do poorly supervised lung nodule identification during training. ng. Instead, people usually look at the EMR picture label while training, which shows whether there are any abnormalities in the CT scan. es. We also take into account supplementary data from EMR, such as the total number of nodules (k) and their respective CT slice indices, in our study. our suggested deep learning architecture for poorly supervised lung nodule detection (Fig. 1) To extract the preliminary prediction (i.e., features, bounding box position) of each nodu, the 3D feature pyramid network (FPN) [1] is used, as illustrated in Fig. 1, with a $\mathbb{H} = ni = ki$, $dБi$ i=1 M pre-trained nodule. All of the aforementioned weak EMR labels—image label y, nodule number k, and nodule slice index z—were used to train our framework, and the prediction outputs are like crude nodule suggestions. my k.

Pulmonary nodule detection with supervision

For object recognition in unsupervised environments, when training is based simply on image-level labels, multiple instance learning (MIL) [4] has been used in the past. The approach mentioned above is designed to estimate nodule suggestions $\mathbb{H}$, which would be correctly linked to the image-level label y, without collecting any labels at the instance level. The feature maps from the 3D-FPN backbone detector, represented as $\mathbb{F} = f<i$ i=1 M, are extracted using the pooling procedure for every proposal $\mathbf{b}i$. One research [5] used completely linked layers activated by a rectified linear unit (ReLU) to deduce the confidence score of each item proposition. Lastly, many methods have been suggested for processing the predicted y from $\mathbb{H}$ in order to align it with the ground-truth image-level prediction [6-8]. As the MIL pooling function, we followed and regarded the maximal operator in our work.

$$\hat{y} = max\{\hat{h}_i\}_{i=1}^{M} = max\{MIL(\hat{f}_i)\}_{i=1}^{M} \quad (1)$$

Throughout the suggested learning framework, h i represents the expected score of the proposals, and MIL stands for the MIL branch. Our weakly supervised pulmonary nodule identification module received the extracted visual features as input, and we didn't change the original ResNet-18's weights.or Backbones of FPN devices. Because of this, we were able to zero down on the network modules responsible for rating and forecasting nodule suggestions that were extracted under various forms of inadequate monitoring.Lung Image.DatabaseConsortiumimagecollection(LIDCIDRI)(https://wiki.cancerimagingarchive.net/plugins/servlet/mobile?contentId=1966254#content/view/1966254,which contains 1018 CT volumes from 1010 distinct patients, was used to pre-train ResNet 18. With 670 scans from seven distinct GE Medical Systems LightSpeed models, 74 scans from four distinct Philips Brilliance models, 205 scans from five distinct Siemens Definition, Emotion, and Sensation models, and 69 scans from a Toshiba Aquilion scanner, there was a wide range of manufacturers and models represented [9].We used 60 CT volumes from 60 patients, together with other hospital confidential data, to assess the model's performance after training.

Reference standard

We utilized the lung nodules that AI and the majority of clinicians (three or more) understood as

our benchmark. The sensitivity of the physician's labeling system is comparable to that of other AI systems and other doctors. False positives (FPs) are lung nodules that the expert has classified but which are not widely agreed upon by other specialists [10].

Analysis

The overall sensitivity and FP were analyzed.The influence of nodular location (upper, middle, lower; central or peripheral), size, and texture in the CT scan was analyzed.

Results

Demographic characteristics

You may see a summary of the patients' demographic information in Table 1. Age was distributed as 62.6±11.0 years. At 159.8±8.8 cm and 61.1±13.6 kg, respectively, was the average height and weight of the participants. There were 33 girls (55% of the total) and 27 men (45%). Although 12 patients were past smokers and 4 were current smokers, the vast majority of patients did not smoke (N=44, 73.3%). In general, the identification of nodules Figure 2 shows that 60 patients had 266 nodules. In the absence of AI, the sensitivity was 63.1% and the FP was 0.617-0.650/scan (mean 0.634, 95% CI 0.586-0.680) for human physicians. With AI help, physicians' FP ranged from 0.067 to 0.2/scan (mean0.122, 95% CI 0.000-0.261), and their sensitivity was 59.2-77.3% (mean69.8%, 95% CI 50.9-88.6%).

Table 1. Demographic characteristics of the patients

Characteristics		
Age (yrs)		62.6±11.0
BH (cm)		159.8±8.8
BW(Kg)		61.1±13.6
Gender	Male	27 (45%)
	Female	33 (55%)
Smoking	Non-smoking	44 (73.3%)
	Current smoker	4 (6.7%)
	Ex-smoker	12 (20.0%)

Abbreviations: BH, body height; BW, body weight.

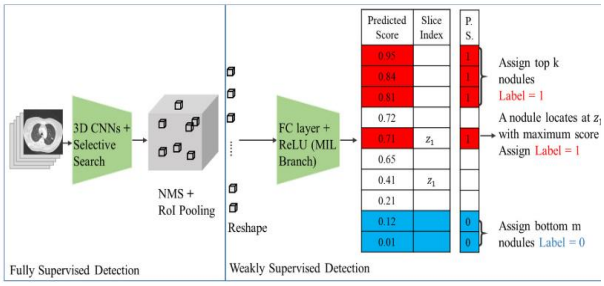

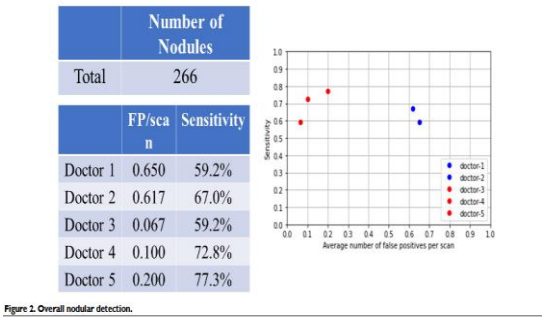

	Number of Nodules
Total	266

	FP/scan	Sensitivity
Doctor 1	0.650	59.2%
Doctor 2	0.617	67.0%
Doctor 3	0.067	59.2%
Doctor 4	0.100	72.8%
Doctor 5	0.200	77.3%

Figure 2. Overall nodular detection.

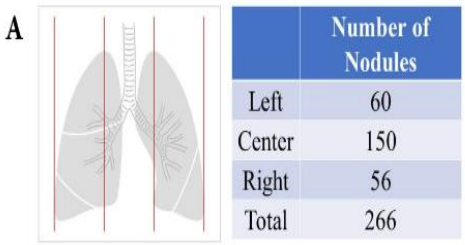

A

	Number of Nodules
Left	60
Center	150
Right	56
Total	266

B

	Left		Center		Right	
	FP/scan	Sensitivity	FP/scan	Sensitivity	FP/scan	Sensitivity
Doctor 1	0.083	63.9%	0.400	50.3%	0.167	77.7%
Doctor 2	0.167	77.9%	0.267	60.8%	0.183	71.2%
Doctor 3	0.000	60.1%	0.067	58.6%	0.000	59.8%
Doctor 4	0.000	75.3%	0.100	71.2%	0.000	73.8%
Doctor 5	0.033	79.5%	0.117	76.9%	0.050	75.6%

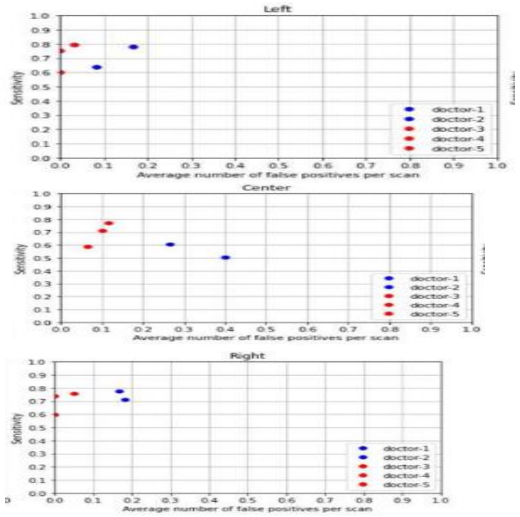

Figure 3. Left, central and right lung fields and nodular detection. Number of pulmonary nodular detection in left, center and right lung fields. False positive and sensitivity of nodular detection in left, center and right lung fields.

Left, central and right lung fields and nodular detection

According to Figure 3A, the number of nodules in the left lung field was 60, in the middle lung area it was 150, and in the right lung field it was 56. Table 2 shows the sensitivity and positive predictive

value (FP) for identifying lung nodules in the left, center, and right lung fields. Without artificial intelligence (AI) support, the sensitivity ranged from 63.9% to 77.9% (mean 70.9%, 95% CI 51.1-90.6%), and the FP for the left lung field was 0.083-0.167/scan (mean 0.125, 95% CI 0.006-0.243) (Fig. 3B). The sensitivity ranged from 60.1% to 75.9% (mean 71.6%, 95% CI), and the FP was 0-0.033/scan (mean 0.011, 95% CI 0.000-0.049) when AI was used. 31.2% to 92.1%. There was an FP of 0.267-8.40/scan (mean 0.334, 95% CI 0.316-0.352) in the central lung areas, and In the absence of AI, the sensitivity ranged from 50.3% to 60.8% (mean 55.6%, 95% CI 40.7-70.3%). The sensitivity was 58.6-76.9% (mean 68.9%, 95% CI 50.1-87.6%), and the FP was 0.067-0.117/scan (mean 0.094, 95% CI 0.043-0.145) with AI aid. Without the use of AI, the sensitivity ranged from 71.2 to 77.7% (mean 74.5, 95% CI 65.2-83.6%) and the FP for the right lung field was 0.167-0.183/scan (mean 0.176, 95% CI 0.153-0.197). The sensitivity ranged from 59.8 to 75.6% (mean 69.7%, 95% CI 52.4-87.0%), and the false positive rate was 0-0.05/scan (mean 0.017, 95% CI 0.000-0.074) when AI was used.

Upper, middle and lower lung fields and nodular detection

In the upper lung fields, 83 nodules were found, in the middle fields, 123 nodules, and in the lower fields, 50 nodules (Fig. 4A). Table 2 displays the comprehensive FP and sensitivity data for the detection of lung nodules in the upper, middle, and lower lung fields. The sensitivity for doctors without AI assistance was 66.5-73.0% (95% CI 60.5-78.9%), while for doctors with AI assistance, the FP ranged from 0.033-0.083/scan (mean 0.055, 95% CI 0.004-0.106), and the sensitivity was 68.3-84.5% (95% CI 60.8-94.2%) for the upper lung fields (Fig. 4B). The FP ranged from 0.100-0.183/scan (mean 0.142, 95% CI 0.024-0.258).The sensitivity for doctors without AI assistance was 52.0-65.0% (mean 58.5%, 95% CI 40.1-76.8%), while for doctors with AI assistance, the sensitivity was 53.9-75.5% (mean 66.1%, 95% CI 43.9-88.2%), and the FP for the middle lung fields was 0.267-0.333/scan (mean 0.300, 95% CI 0.206-0.393). The sensitivity was 45.2-43.9% (mean 44.5%, 95% CI 42.7-46.3%) and the FP was 0.1-0.267/scan for the lower lung fields among clinicians without AI aid; the 95% confidence interval for this range was 0.000-0.419. The sensitivity of physicians with AI aid was 37.4-51.2%, and the FP ranged from 0.017-0.033/scan (mean 0.017, 95% CI 0.000-0.049).

A

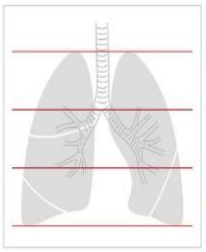

	Number of Nodules
Upper	83
Middle	123
Lower	50
Total	266

B

	Upper		Middle		Lower	
	FP/scan	Sensitivity	FP/scan	Sensitivity	FP/scan	Sensitivity
Doctor 1	0.100	66.5%	0.333	52.0%	0.267	45.2%
Doctor 2	0.183	73.0%	0.267	65.0%	0.100	43.9%
Doctor 3	0.033	68.3%	0.033	53.9%	0.000	37.4%
Doctor 4	0.050	79.9%	0.017	68.9%	0.017	47.7%
Doctor 5	0.083	84.5%	0.050	75.5%	0.033	51.2%

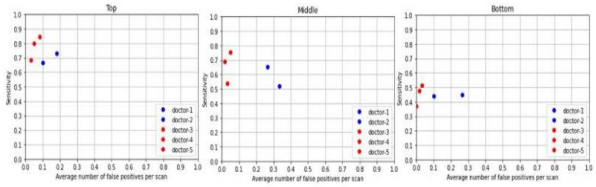

Figure 4. Upper, middle and lower lung fields and nodular detection. (A) Number of pulmonary noular detection in upper, milddle and lower lung fields. (B) False positive and sensitivity of nodular detection in upper, milddle and lower lung fields.

Table 2. The false positive and sensitivity of AI detection in different location, size and texture

		Location						Location					
		Left		Central		Right		Upper		Middle		Lower	
		FP/scan	Sensitivity	FP/scan	Sensitivity	FP/scan	Sensitivity	FP/scan	Sensitivity	FP/scan	Sensitivity	FP/scan	Sensitivity
without AI	mean	0.125	70.9%	0.334	55.6%	0.176	74.5%	0.142	69.8%	0.300	58.5%	0.184	44.5%
	lower 95% CI	0.006	51.1%	0.316	40.7%	0.153	65.2%	0.024	60.5%	0.206	40.1%	0.000	42.7%
	upper 95% CI	0.243	90.6%	0.352	70.3%	0.197	83.6%	0.258	78.9%	0.393	76.8%	0.419	46.3%
with AI	mean	0.011	71.6%	0.094	68.9%	0.017	69.7%	0.035	77.6%	0.033	66.1%	0.017	43.4%
	lower 95% CI	0.000	51.2%	0.043	50.1%	0.000	52.4%	0.004	60.8%	0.003	43.9%	0.000	31.0%
	upper 95% CI	0.049	92.1%	0.145	87.6%	0.074	87.0%	0.106	94.2%	0.066	88.2%	0.049	59.7%
		Size						Texture					
		Small		Middle		Large		GGO		Partial solid		solid	
		FP/scan	Sensitivity	FP/scan	Sensitivity	FP/scan	Sensitivity	FP/scan	Sensitivity	FP/scan	Sensitivity	FP/scan	Sensitivity
without AI	mean	0	3.2%	0.192	69.4%	0.442	80.2%	0.409	65.1%	0.100	74.6%	0.125	57.9%
	lower 95% CI	0	3.2%	0.000	40.3%	0.041	77.4%	0.101	64.7%	0.000	61.3%	0.102	39.5%
	upper 95% CI	0	3.2%	0.543	98.3%	0.841	82.8%	0.713	65.5%	0.334	87.8%	0.147	76.2%
with AI	mean	0.077	76.3%	0.011	80.3%	0.033	59.3%	0.039	61.5%	0.056	74.5%	0.078	74.7%
	lower 95% CI	0.000	57.5%	0.000	67.3%	0.000	35.3%	0.000	43.6%	0.000	63.6%	0.000	51.6%
	upper 95% CI	0.177	94.9%	0.030	93.3%	0.066	83.3%	0.108	79.3%	0.219	85.2%	0.173	97.7%

A

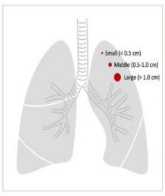

	Number of Nodules
Small (<0.5cm)	43
Middle (0.5-1.0cm)	94
Large (>1.0cm)	129
Total	266

B

	Small		Middle		Large	
	FP/scan	Sensitivity	FP/scan	Sensitivity	FP/scan	Sensitivity
Doctor 1	0.000	3.2%	0.067	59.1%	0.583	81.1%
Doctor 2	0.000	3.2%	0.317	79.6%	0.300	79.2%
Doctor 3	0.030	67.6%	0.000	72.9%	0.033	45.8%
Doctor 4	0.070	75.0%	0.017	83.1%	0.017	63.5%
Doctor 5	0.130	86.2%	0.017	85.0%	0.050	68.7%

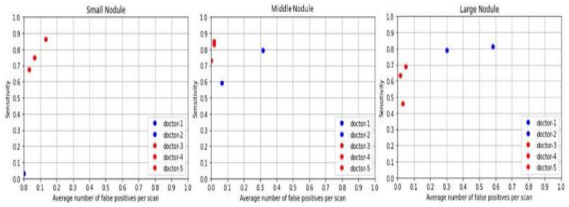

Figure 5. Nodular size and nodular detection. (A) Number of difference sizes of pulmonary nodules. (B) False positive and sensitivity of nodular detection in difference sizes of pulmonary nodules.

Nodular size and nodular detection

The number of nodules was as follows: 43 tiny nodules, 94 intermediate nodules, and 129 big nodules, with diameters ranging from less than half a centimeter to more than one centimeter (Fig. 5A). Table 2 displays the sensitivity and FP for identifying lung nodules of varying sizes. With regard to the tiny nodules, the FP was 0.003-0.13/scan (mean 0.077, 95% CI 0.000-0.177), the sensitivity was 64.6-86.2% (mean 76.3%, 95% CI 57.5-94.9%) among physicians who used AI, and the FP was 0 (mean 0, 95% CI 0-0) among doctors who did not.support (Figure 5B). For the middle nodules, the FP ranged from 0.067 to 0.317/scan (mean 0.192, 95% CI 0.000-0.545), with a sensitivity of 59.1-79.6% (mean 69.4%, 95% CI 40.3-98.3%) for doctors without AI assistance, and from 0-0.017/scan (mean 0.011, 95% CI 0.000-0.030) for doctors with AI assistance, with a sensitivity of 72.9-85.0% (mean 80.3%, 95% CI 67.3-93.3%). The sensitivity for doctors without AI assistance was 79.2-81.1% (mean 80.2%, 95% CI 77.4-82.8%) for large nodules, while for doctors with AI assistance, the sensitivity was 45.8-68.7% (mean 59.3%, 95% CI 35.3-83.3%) and the FP was 0.3-0.583/scan (mean 0.442, 95% CI 0.041–0.841). Texture of nodules and detection of nodules .The number of ground-glass organization (GGO) nodules was 109, with 41 being partial and 116 being solid (Fig. 6A). The sensitivity and FP for identifying lung nodules with various nodular textures are summarized in Table 2. Without AI support, the sensitivity for GGO nodule detection was 65.1% and the FP ranged from 0.3-0.517/scan (95% CI 0.101-0.715). The sensitivity ranged from 52.2% to 70.0% (mean 61.5%, 95% CI 43.6-79.3%), and the FP was 0-0.067/scan (mean 0.039, 95% CI 0.000-0.108) among clinicians who used AI (Fig. 6B). In the case of partial solid nodules, the FP ranged from 0.017 to 0.183/scan (95% CI 0.000-0.334), with a sensitivity of 69.9-79.3% (mean 74.6%, 95% CI 61.3-87.8%) among doctors who did not use AI. In contrast, the FP ranged from 0-0.150 (mean 0.056, 95% CI 0.000-0.219), with a sensitivity of 68.3-78.4% (mean 74.5%, 95% CI 63.6-85.2%) among doctors who did use AI. Concerning the solid nodules, the FP ranged from 0.117 to 0.133/scan (mean 0.125, 95% CI 0.102-0.147), with a sensitivity of 51.4-64.4% (mean 57.9%, 95% CI 39.5-76.2%) among doctors who did not have access to AI. In contrast, the FP ranged from 0.050-0.133/scan (mean 0.078, 95% CI 0.000-0.173), and among doctors who did have access to AI, the sensitivity ranged from 51.2-63.5% (mean 74.7%, 95% CI 51.6-97.7%).

A

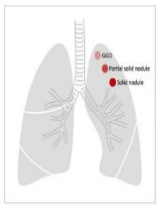

	Number of Nodules
GGO	109
Part Solid	41
Solid	116
Total	266

B

	GGO		Part Solid		Solid	
	FP/scan	Sensitivity	FP/scan	Sensitivity	FP/scan	Sensitivity
Doctor 1	0.517	65.3%	0.017	69.9%	0.117	51.4%
Doctor 2	0.300	65.0%	0.183	79.3%	0.133	64.4%
Doctor 3	0.000	52.2%	0.017	68.3%	0.050	61.5%
Doctor 4	0.050	62.4%	0.000	76.7%	0.050	79.8%
Doctor 5	0.067	70.0%	0.150	78.4%	0.133	82.8%

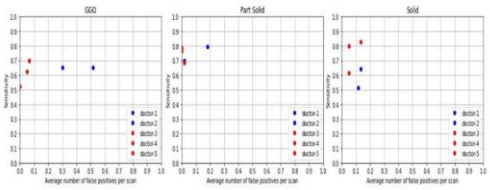

Figure 6. Nodular texture and nodular detection. Number of difference textures of pulmonary nodules. False positive and sensitivity of nodular detection in difference textures of pulmonary nodules.

Discussion

In this investigation, we locate a number of noteworthy things. Predictions about the center and middle locations are more likely to be FP and less sensitive when doctors are not supported by AI. The doctor's sensitivity is low while dealing with little nodules in the lungs (less than half a centimeter). Medical professionals were more likely to have FP for GGOs when considering nodule texture. The doctor's sensitivity and total rate of false positives may be enhanced with the help of AI. There is room for improvement in the precision of the aforementioned aspects or regions.One plausible concern is that AI or medical professionals may fail to detect lung nodules if they are too little. According to prior research, the tiny size of CT images is the leading cause of missed diagnoses [11]. One of the reasons for a failure diagnosis, according to Del Ciello et al. [11], might be a tiny diameter (<7 mm). Our research found that manually detecting small nodules (<0.5 cm) in chest CT images was very challenging, with a sensitivity of just 3.2%. The sensitivity detecting small nodules was substantially enhanced with the use of AI. A number of studies have also shown that using AI as an additional reader greatly improves the sensitivity of detecting lung nodules [12]. Lung nodules' central placement is a

contributing factor to their being overlooked [11]. There is an abnormally high incidence of central lung nodule missingness, according to Del Ciello et al. [11]. One of the reasons lung tumors might go undetected is hilar nodules, which are blind regions on CT scans (Deveraj et al., 2013). On computed tomography (CT) scans, some healthy tissues could pass for nodules. In particular, around the hilar region, more normal lung tissues are located in the middle. When diagnosing lung nodules, clinicians may have trouble telling them apart from other structures, such as pulmonary arteries and bones [11]. There will be a drop in accuracy due to the challenges in interpretation caused by this. An increase in FP occurs when lung tissues are seen as nodules in the lungs.On the other side, the sensitivity will be diminished if the preexisting lung nodules are considered lung tissues. Therefore, in order to decrease FP in an automated lung nodule identification system, the method for distinguishing between tissues and nodules is critical [1]. The FP rates were significantly reduced in our AI helper projects. A CT scan's ability to identify lung nodules depends in part on the nodules' unique features.Lung tumors that go undetected by CT scans are often extremely tiny and hardly perceptible, as previously shown by Li et al. [14]. Additionally, Del Ciello et al. demonstrated that imprecise or hazy borders contribute to the omission of lung nodules [11]. Software identification of attenuation differences with the surrounding parenchyma may be impeded by the ground-glass component, according to Benzakoun et al. [15]. A sensitivity of 72% for partly solid nodules was shown to be much superior than 28% for pure ground-glass nodules [15]. We found a happy medium between sensitivity and FP in our investigation as compared to others. Prior research has shown good identification sensitivity, albeit at the expense of rather high FP rates. The deep learning technique developed by Cui et al. [10] demonstrated a sensitivity of 91.0% but had 2FPs/case, and it was trained on a large multi-center database using a 50-layer neural network. An overall accuracy of 64.4% was shown using the computer-aided detection techniques presented by Ali et al. [16]. The specificity was 55.3%, sensitivity was 58.9%, PPV was 54.2%, and NPV was 60.0%. Using their 3D-convolutional neural network (CNN), Cao et al. achieved 90% sensitivity and FP 1/scan [17]. Similar to Setio et al., who employed multiview convolutional networks to achieve a sensitivity of 90.1% and 4 FPs/case [19], Dou et al. similarly used 3D CNNs and demonstrated a sensitivity of 90.7% and 4 FPs/case [18]. The findings demonstrated a high level of sensitivity, but they also had a rather high proportion of false positives, ranging from two to four per scan [10, 16, 17, 19].It is critical to strike a balance between sensitivity and FP. When it came to CT screening for lung nodules utilizing computer-aided detection, the majority of earlier models had good sensitivity and FP. These days, specialists can find localized lung lesions much more quickly thanks to technological advancements. Unfortunately, false positives (FP) induce needless follow-up testing and costs, making them a major issue in lung nodule detection [16]. As a result, patients endure more pain and may have to undergo invasive treatments that aren't needed to confirm the diagnosis. Because of this, the danger of procedures is higher. Another possible cause of radiation-induced cancer is the need for routine and frequent follow-up chest CT scans [20]. Moreover, prior research has shown that computer-aided detection software has high FP, which poses a significant barrier to the system's broader use [11]. Consequently, the majority of computer-assisted detection systems fail to provide tangible advantages when put into practice [20]. AI lung nodule detection has a serious difficulty with FP reduction.Our AI-assisted approach significantly lowers the FP rate and boosts clinicians' efficiency in the present investigation.

Limitations of the study

Our AI-assisted model enhanced the accuracy of interpreting CT scans and the job efficiency of physicians. However, this research has several drawbacks. First, this study concentrated on the identification of lung nodules, but did not focus on the separation of benign and cancerous nodules. We did not examine the performance of the lung cancer utilizing the present model.Therefore, such an aide system needs more study to validate the diagnosis of lung cancers.However, via early diagnosis of tiny lung nodules, we think that early identification of lung cancer is still helpful.Secondly, there isn't a gold dust norm is a typical issue with AI identification of masses in the lungs [10]. The results of a lung nodule biopsy can verify the validity, however,this is usually not possible. The majority opinion of professionals was used in this investigation. for use as a benchmark. This method was comparable to prior research on artificial intelligence for the diagnosis of lung benign growths [10]. Finally, lung nodule incidence changes depending on the study's unique attributes population, such as race, age, and smoking status. Hence, AI's precision varies for various groups of people [10, 20]. Our present system still needs to be utilized in different ethnic groupings.

Conclusions

The medicolegal ramifications of physicians missing lung cancer are substantial. Some of the characteristics of the undiscovered lesion—its tiny size, ground-glass appearance, and central location—are associated with the grounds for CT scan mistake. When dealing with a high number of

CT images, manual detection is laborious, error-prone, time-consuming, and demands a lot of attention from clinicians. Our research found that AI helper programs reduced the occurrence of misdiagnosis of lung nodules in the error-prone features of these lessions.Thank You Notes Foundation for Buddhist Tzu Chi Medicine and Taipei Tzu Chi Hospital (TCRD-TPE-109-24(2/3)) provided funding for this research. Conflicting Priorities There is no conflict of interest, as the writers have stated.

References

1. Liu J, Cao L, Akin O, et al. Accurate and robust pulmonary nodule detection by 3D feature pyramid network with self-supervised feature learning. arXiv.2019; 1907:11704.

2. Dziedzic R, Marjański T, Rzyman W. A narrative review of invasive diagnostics and treatment of early lung cancer. Transl Lung Cancer R. 2021; 10(2):1110-23.

3. Morozov SP, Gombolevskiy VA, Elizarov AB, et al. A simplified cluster model and a tool adapted for collaborative labeling of lung cancer CT scans. Comput Meth Prog Bio. 2021; 206:106111.

4. Chikontwe P, Kim M, Nam SJ, et al. Multiple instance learning with center embeddings for histopathology classification. MICCAI. 2020.

5. Ilse M, Tomczak J, Welling M. Attention-based deep multiple instance learning. ICML. 2018.

6. Sadafi A, Makhro A, Bogdanova A, et al. Attention based multiple instance learning for classification of blood cell disorders. MICCAI. 2020;1-11.

7. Xu G, Song Z, Sun Z, et al. Camel: A weakly supervised learning framework for histopathology image segmentation. IEEE/CVF International Conference on Computer Vision (ICCV). 2019;10681–90.

8. Bilen H, Vedaldi A. Weakly supervised deep detection networks. CVPR. 2019;2846–54.

9. Hancock MC, Magnan JF. Lung nodule malignancy classification using only radiologist-quantified image features as inputs to statistical learning algorithms: probing the Lung Image Database Consortium dataset with two statistical learning methods. J Med Imaging (Bellingham). 2016; 3(4):044504.

10. Cui S, Ming S, Lin Y, et al. Development and clinical application of deep learning model for lung nodules screening on CT images. Sci Rep. 2020;10(1):13657.

11. Del Ciello A, Franchi P, Contegiacomo A, et al. Missed lung cancer: when, where, and why? Diagn Interv Radiol. 2017; 23(2):118-26.

12. Zhao Y, de Bock GH, Vliegenthart R, et al. Performance of computer-aided detection of pulmonary nodules in low-dose CT: comparison with double reading by nodule volume. Eur Radiol. 2012;22(10):2076-84.

13. Devaraj A. Missed cancers in lung cancer screening--more than meets the eye. Eur Radiol. 2015; 25(1):89-91.

14. Li F, Sone S, Abe H, et al. Lung cancers missed at low-dose helical CT screening in a general population: comparison of clinical, histopathologic, and imaging findings. Radiology. 2002; 225(3):673-83.

15. Benzakoun J, Bommart S, Coste J, et al. Computer-aided diagnosis (CAD) of subsolid nodules: Evaluation of a commercial CAD system. Eur J Radiol. 2016; 85(10):1728-34.

16. Ali I, Hart GR, Gunabushanam G, et al. Lung Nodule Detection via Deep Reinforcement Learning. Front Oncol. 2018; 8:108.

17. Cao H, Liu H, Song E, et al. A Two-Stage Convolutional Neural Networks for Lung Nodule Detection. IEEE J Biomed Health Inform. 2020; 24(7):2006-15.

18. Dou Q, Chen H, Yu L, et al. Multilevel Contextual 3-D CNNs for False Positive Reduction in Pulmonary Nodule Detection. IEEE Trans Biomed Eng. 2017;64(7):1558-67.

19. Setio AA, Ciompi F, Litjens G, et al. Pulmonary Nodule Detection in CT Images: False Positive Reduction Using Multi-View Convolutional Networks. Ieee T Med Imaging. 2016; 35(5):1160-9.